Microchim Acta
DOI 10.1007/s00604-014-1355-x

ORIGINAL PAPER

Electrochemical immunosensing using a nanostructured functional platform for determination of α-zearalanol

Matías Regiart · Marco A. Seia · Germán A. Messina · Franco A. Bertolino · Julio Raba

Received: 9 June 2014 / Accepted: 1 September 2014

Abstract We describe an electrochemical immunosensor for the determination of the growth promoter α-zearalanol in bovine serum. The sensing scheme is based on a nanocomposite consisting of gold nanoparticles electrodeposited on multi-walled carbon nanotubes that were modified with poly (vinylpyridine) through *in-situ* polymerization. The electrodeposition of the gold nanoparticles enlarges the surface available for immobilization of antibodies against α-zearalanol. The nanocomposite film was characterized by scanning electron microscopy, energy dispersive X-ray spectroscopy, and cyclic voltammetry. The calibration plot has a linear response in the concentrations range from 0.05 to 50 ng mL^{-1}, and the detection limit is 16 pg mL^{-1}. The time required for analysis is 12 min only which compares quite favorably with the time (90 min) required by the conventional ELISA. The method exhibits good selectivity, stability and reproducibility for detecting α-zearalanol in the livestock production.

Keywords Electrochemical · Immunosensor · Nanocomposite · α-zearalanol · Bovine serum

Introduction

α-zearalanol (ZEN) is a non-steroidal estrogenic agonist generated by chemical reduction of the mycotoxin zearalenone, which is produced by *Fusarium spp* and it is commonly found in contaminated grain products [1, 2]. ZEN belongs to the resorcylic acid lactones family [3], and it has been widely used as growth promoter in the livestock production [4]. Previous studies have shown their potential risk factor for breast cancer, with strong and prolonged endocrine-disruptive effects in humans at very low concentrations [5]. Compounds identified as endocrine disrupting compounds (EDCs) are members of different groups of chemicals, including drugs, pesticides, industrial products, alkylphenols, synthetic steroids, and so on [6]. ZEN is a member of EDCs and its administration as a growth promoter has been banned in the European Union since 1985 [7].

Different methods have been reported for the determination of EDCs in biological samples, such as capillary electrophoresis-amperometric detection [8], liquid chromatography-mass spectrometry [9], ultra high performance liquid chromatography-mass spectrometry [10], gas chromatography–mass spectrometry [11] and biosensors [12]. Immunoassay techniques, which are based on the highly specific molecular recognition of antigens by antibodies, have become important analytical methods in clinical, biochemical, pharmaceutical and environmental fields [13]. In recent years, electrochemical immunosensors have gained interest because of their high sensitivity, low detection limit, fast analysis and low cost of the instrumentation [14–16]. Screen-printing is one of the most promising approaches towards simple, rapid and inexpensive production of biosensors. Screen-printed technology has advantages of design flexibility, process automation, good reproducibility, a wide choice of materials [17].

Since the discovery of carbon nanotubes (CNTs) in 1991 by Ijima [18], there have emerged several modification methods with the aim of use them as immobilization platform. Most of these strategies alter the structural and functional properties of CNTs due to the extensive and strong chemical treatments that they are subjected [19]. For this reason, the use

Electronic supplementary material The online version of this article (doi:10.1007/s00604-014-1355-x) contains supplementary material, which is available to authorized users.

M. Regiart · M. A. Seia · G. A. Messina · F. A. Bertolino (✉) · J. Raba (✉)
INQUISAL-CONICET, Departamento de Química, Universidad Nacional de San Luis, Chacabuco, 917, D5700BWS San Luis, Argentina
e-mail: bertolin@unsl.edu.ar
e-mail: jraba@unsl.edu.ar

Published online: 11 September 2014

of polymerization methods not only maintain the nanotubes properties such as high chemical and mechanical stability, high conductivity, high specific surface area [20], but also incorporate a high biocompatibility, hydrophilicity, stability and permeability of the new material. These types of strategies used the polymerization of a monomer in the presence of CNTs, forming a uniform framework that shows the same physicochemical properties in each point of the framework [21].

In this way, the multi-walled carbon nanotubes (MWCNTs) modified with poly (vinylpyridine) (PVP) offer a large specific surface area with high chemical stability and mechanical strength. MWCNTs improve the conductivity of the prepared nanocomposite film [22]. The chemical functionalization of MWCNTs is important not only to increase their dispersion, but also to facilitate their interaction with organic and biological molecules [23]. Moreover, the porous three dimensional films could provide a high accessible surface area and good biocompatible microenvironment for immobilization of antibodies [24]. In recent years, noble metal nanoparticles, with extraordinary conductivity, large surface-to-volume ratio and biocompatibility, have been extensively employed for developing novel electrochemical sensing platforms and improving their performances [25]. Based on the foregoing, the electrodeposition of gold nanoparticles (AuNPs) on these platforms have many properties such as high active surface for antibodies immobilization, facilitate the electron transfer due to their good conductivity, excellent film-forming ability, high water permeability, good adhesion, nontoxicity and remarkable biocompatibility [26–28].

To the best of our knowledge, no study involving the construction and characterization of a nanostructured functional platform on portable screen-printed carbon electrode (SPCE) for the immunocapture of ZEN and its subsequent determination by square-wave voltammetry (SWV) has been reported. Therefore, in this article, we present and discuss a novel nanocomposite based on MWCNTs-PVP with AuNPs electrodeposited, applied to the sensitive and selective determination of ZEN in bovine serum.

Materials and methods

Reagents

All reagents used were of analytical reagent grade. ZEN, bovine serum albumin (BSA, 98 %), 3-mercaptopropionic acid (MPA), N-(3-dimethylaminopropyl)-N-ethylcarbodiimide (EDC), N-hydroxysuccinimide (NHS), $HAuCl_4$ 0.01 %, azobis (isobutyronitrile) (AIBN), multi-walled carbon nanotubes (90 % purity, 10–15 nm external diameter, 2–6 nm internal diameter, 0.1–10 μm length), 4-vinylpyridine, potassium ferrocyanide, potassium ferricyanide and N,N-dimethylformamide (DMF) were purchased from Sigma Aldrich (St. Louis, MO, USA, http://www.sigmaaldrich.com). Polytetrafluoroethylene membrane (PTFE) (0.2 μm) was obtained from Millipore (Billerica, MA, USA, http://www.millipore.com). Rabbit anti-ZEN antibody was purchased from CER GROUP (Marloie, Belgium, http://www.cergroupe.be/en). All other reagents and solvents employed were of analytical grade and they were used without further purifications. All solutions were prepared with ultra-high-quality water obtained from a Barnstead Easy pure RF compact ultra-pure water system.

Equipment

Scanning electron micrographs were obtained using a LEO 1450VP scanning electron microscope (SEM, http://labmem.unsl.edu.ar). The elemental composition of the nanostructured film was determined by energy dispersive X-ray spectroscopy (EDS, http://labmem.unsl.edu.ar) using a Genesis 2000 spectrometer. Cyclic voltammetry (CV) and square wave voltammetry (SWV) measurements were performed using a BAS 100 B/W (electrochemical analyzer Bioanalytical System, West Lafayette, IN, http://www.basinc.com). A SPCE made up of three electrodes was used. A silver ink as pseudo-reference electrode, a graphite ink as auxiliary electrode and, a graphite ink circular (Ø=3 mm) with and without modifications as working electrode were used for all the measurements (DropSens, Llanera, Asturias, Spain, http://www.dropsens.com). All solutions and reagents were conditioned to 25±1 °C before the experiment, using a laboratory water bath (Vicking Mason II, Vicking SRL, Argentina, http://www.vicking.com.ar). Absorbance was detected by a Bio-Rad Benchmark microplate reader (Japan, http://www.bio-rad.com) and Beckman DU 520 general UV/vis spectrophotometer (http://www.beckmancoulter.com). All pH measurements were made with an Orion expandable ion analyzer Model EA 940 equipped with a glass combination electrode (Orion Research Inc., http://www.bioesanco.com.ar).

Construction of the AuNPs/MWCNTs-PVP functional platform on SPCE

In order to obtain the nanocomposite of MWCNTs polymerized with PVP, we used the procedure described by Silva et al. [22] with the following modifications. In a 50 mL flask containing 40 mL of DMF were added 50 mg of MWCNTs under nitrogen atmosphere and the mixture was stirred for 15 min. Afterwards, 70 mg of AIBN and 10 mL of 4-vinylpyridine were added. The solution was placed in a thermostated oil bath at 80 °C under stirring for 48 h. After this period, the mixture was cooled to room temperature and diluted to 250 mL with DMF. The supernatant was centrifuged for 6 h and vacuum-filtered through a 0.20 μm PTFE membrane.

To obtain the dispersion of MWCNTs-PVP nanocomposite, the following procedure was employed: 6 mg of the nanocomposite was dispersed in 1 mL DMF and ultra sonicated for 2 h in order to obtain a homogeneous suspension. An aliquot of 2.5 μL of this dispersion was added to the SPCE and then, the electrode was dried at room temperature.

For the electrodeposition procedure of AuNPs, the SPCE was immersed into 0.01 % $HAuCl_4$ solution containing 0.1 mol L^{-1} KCl (prepared in doubly distilled water and deaerated by bubbling with nitrogen) as supporting electrolyte. After that, a constant potential value of −0.4 V was applied for 30 s. Then, the modified electrode was rinsed with doubly distilled water and dried carefully with pure nitrogen gas. Finally, the AuNPs/MWCNTs-PVP/SPCE was optimized and characterized by SEM, EDS and CV.

Preparation of anti-ZEN-AuNPs/MWCNTs-PVP/SPCE

After obtaining the AuNPs/MWCNTs-PVP/SPCE, it was placed in contact with MPA 0.04 mol L^{-1} in $EtOH/H_2O$ (75:25, v/v) for 15 h at room temperature. At this point, the -SH group of MPA reacted with the surface of AuNPs previously electrodeposited, leaving as a result free -COOH groups, which were activated by rinsing in a solution containing EDC and NHS in 0.01 mol L^{-1} phosphate buffered saline (PBS) pH 7.20, and then evaporated to dryness. After that the electrode was rinsed with doubly distilled water and dried with pure nitrogen gas. Finally, a solution of anti-ZEN 1/500 in 0.01 mol L^{-1} PBS pH 7.20 was placed on the surface of the AuNPs/MWCNTs-PVP/SPCE working electrode and incubated overnight at 4 °C. After that, the immunosensor was rinsed with 0.01 mol L^{-1} PBS pH 7.20 and stored at 4 °C in the same buffer when not in use. Scheme 1 shows the procedure of the immunosensor preparation.

Procedure for immunocapture and detection of ZEN

This method was applied to the determination of ZEN in bovine serum using a micro-volume electrochemical cell. Prior to the analysis of each serum sample, the unspecific binding of the modified AuNPs/MWCNTs-PVP/SPCE working electrode was blocked by 2 min treatment of 500 μL 1 % BSA in a 0.01 mol L^{-1} PBS pH 7.20 and then washed several times with 500 μL of 0.01 mol L^{-1} PBS pH 7.20. The serum samples were first diluted 50-fold with 0.01 mol L^{-1} PBS pH 7.20 and then 200 μL was added to the immunosensor for 5 min. In this step, the ZEN present in the sample binds immunologically to the anti-ZEN antibodies. Then, the immunosensor was washed three successive times with 0.01 mol L^{-1} PBS pH 7.20. Finally, the electrode was placed in 100 μL of desorption buffer (0.1 mol L^{-1} glycine-HCl pH 2.0) where ZEN was desorbed on the modified electrode surface and it was oxidized at +1.12 V. A standard curve for the immunosensor was produced following our protocol with a series of standards that covered the relevant range (0–100 ng mL^{-1}) supplied with the ELISA test kit. When not in use, the immunosensor was stored in 0.01 mol L^{-1} PBS pH 7.20 at 4 °C. Scheme 2 shows the procedure for immunocapture and detection of ZEN.

Results and discussion

Characterization of the AuNPs/MWCNTs-PVP/SPCE

Morphologies of SPCE, MWCNTs/SPCE MWCNTs-PVP/SPCE and AuNPs/MWCNTs-PVP/SPCE nanocomposite films were investigated by SEM. Figure 1a shows the bare graphite carbon surface. Figure 1b reveals that MWCNTs are well distributed on the SPCE surface and, Fig. 1c shows the change in the morphology of MWCNTs due to the presence of PVP, indicating that PVP was successfully polymerized over the nanomaterial. In addition, Fig. 1d reveals that the electrodeposition of AuNPs onto the nanocomposite film not modified the morphology of this material. The three-dimensional structure of AuNPs/MWCNTs-PVP nanocomposite film provides a suitable surface for anti-ZEN antibodies

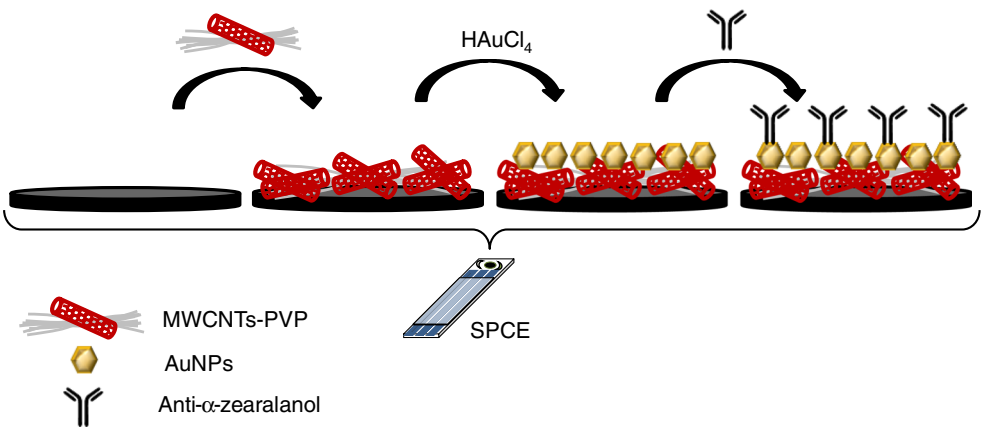

Scheme 1 Procedure for the anti-ZEN-AuNPs/MWCNTs-PVP/SPCE preparation

Scheme 2 Procedure for immunocapture and detection of ZEN

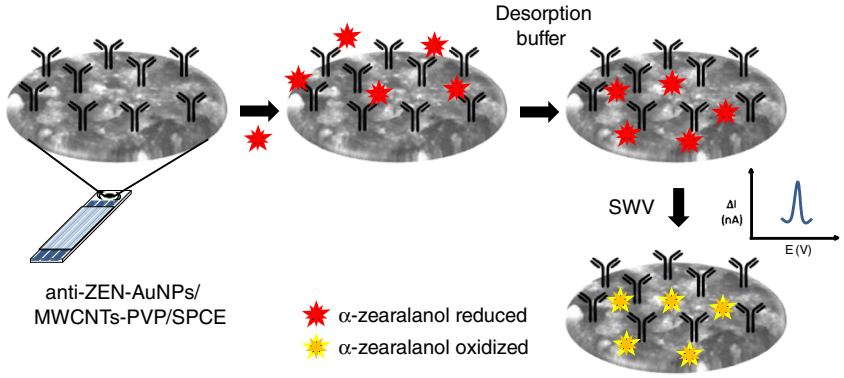

immobilization and a conductive pathway for electron-transfer. The elemental composition of the nanocomposite was determined by EDS. Figure 1e shows the three peaks of interest, at 0.3, 2.3 and 9.8 keV, corresponding to the C and Au atoms, respectively.

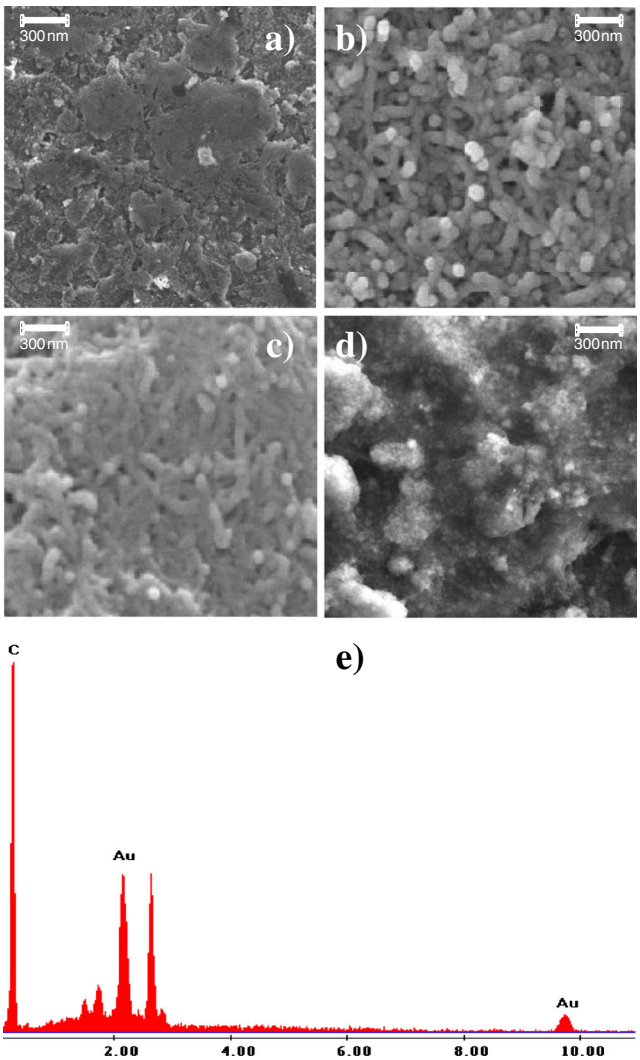

Fig. 1 Morphology characterization of AuNPs/MWCNTs-PVP/SPCE nanocomposite. The morphologies of **a**) SPCE, **b**) MWCNTs/SPCE **c**) MWCNTs-PVP/SPCE and **d**) AuNPs/MWCNTs-PVP/SPCE nanocomposite films were investigated by SEM. **e**) The elemental composition of the nanocomposite was determined by EDS

Electrochemical response of the AuNPs/MWCNTs-PVP/SPCE

Figure 2 shows the CV of modified and unmodified SPCE for 1 mmol L^{-1} ferrocyanide/ferricyanide redox couple solution, containing 0.1 mol L^{-1} KCl solution from −0.2 to + 0.8 V at a scan rate of 75 mV s^{-1}. Well-defined CVs and characteristic diffusion-controlled redox process were observed at the SPCE surface (black line). The red line illustrates the voltammetric effect of the redox couple on the MWCNTs-PVP film. When the dispersion of MWCNTs-PVP was deposited on the electrode surface, the peak current was larger than the observed for bare SPCE, indicating that the nanocomposite improved the conductivity and increased the active surface area of the electrode. When AuNPs/MWCNTs-PVP was used (blue line), the highest peak current was obtained, due to the large surface area of AuNPs and MWCNTs. The average value of surface area for AuNPs/MWCNTs-PVP/SPCE was 12.65 (±0.15)× 10^{-2} cm^2 (n=6) according to the Randles-Sevick equation, that is $I_p=2.69\times10^5\ AD^{1/2}\ n^{3/2}\ \nu^{1/2}\ C$.

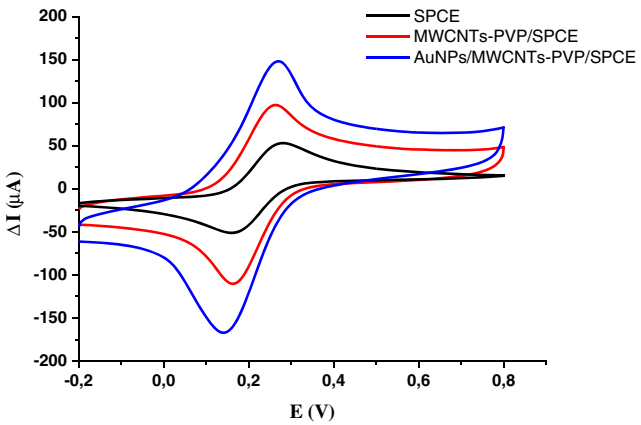

Fig. 2 Electrochemical characterization of the different modified electrodes. CVs were performed in 1 mmol L^{-1} $K_3[Fe(CN)_6]/K_4[Fe(CN)_6]$ in 0.1 mol L^{-1} KCl (pH 6.50) solution from −0.2 to +0.8 V at a scan rate of 75 mV s^{-1}

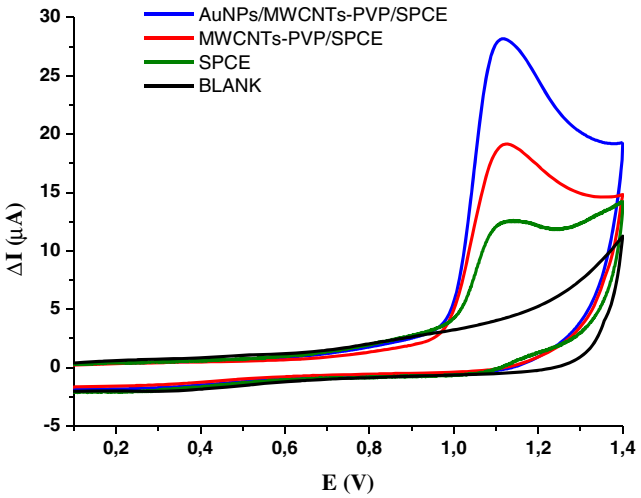

Fig. 3 Electrochemical behavior of 1 mmol L^{-1} ZEN in 0.1 mol L^{-1} glycine-HCl (pH 2.0) with different modified electrodes

Electrochemical behavior of ZEN on AuNPs/MWCNTs-PVP/SPCE

After performing the electrochemical characterization of modified electrodes, the ZEN behavior was studied with modified electrodes by CV as shown in Fig. 3. The figure shows a typical voltammogram of 1 mmol L^{-1} ZEN in 0.1 mol L^{-1} glycine-HCl pH 2.0 solution as supporting electrolyte (scan rate = 75 mV s^{-1}; T=25±1 °C). The cyclic voltammogram showed a single anodic peak at E_{pa} = +1.12 V for the potential range +0.1 to +1.4 V, which corresponded to the one-electron transfer of ZEN. When the sweep was performed in the reverse direction, no reduction peak was observed, showing that the ZEN oxidation is an irreversible process at the surface electrode under the experimental conditions. As can be seen in Fig. 3, the modification of the electrode surface with AuNPs/MWCNTs-PVP nanocomposite increased the oxidation peak current and hence, the sensitivity of the method.

Election of the electroanalytical technique

The immunocapture of ZEN on the anti-ZEN-AuNPs/MWCNTs-PVP/SPCE was an efficient method for the determination of very low levels of ZEN in real samples. The ZEN bound to the immunosensor could be desorbed and directly measured in 0.1 mol L^{-1} glycine-HCl buffer at pH 2.0. The SWV has several advantages compared to other electroanalytical techniques such as, high sensitivity, great speed of analysis, low consumption of the electroactive species and reduction of the problems with the poisoning of the electrode surface. For this reason, the electrochemical sensing of ZEN in bovine serum was carried out using SWV by direct measurement of its oxidation peak after desorption of the immunosensor.

Optimization of experimental conditions

In order to perform the electrochemical sensing of ZEN in bovine serum, many variables that affect the electrochemical

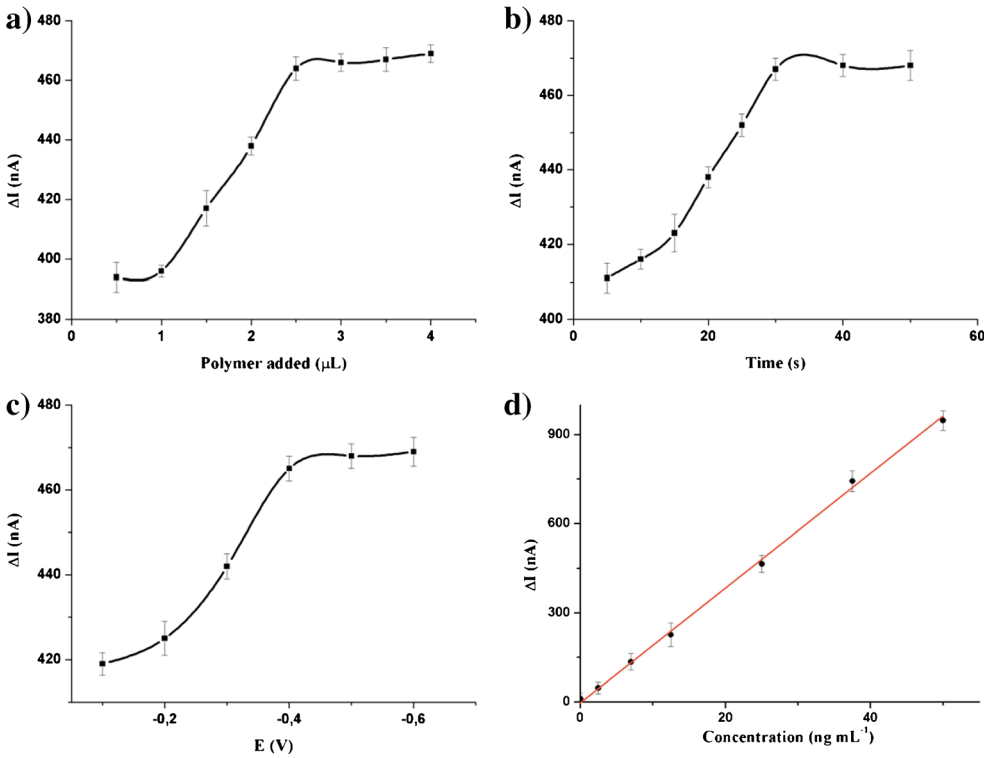

Fig. 4 Optimization of experimental conditions. **a**) The amount of polymer deposited on the electrode, **b**) the electrodeposition time of AuNPs, **c**) the electrodeposition potential of AuNPs, and **d**) the calibration curve for ZEN was obtained in a linear range from 0.05 to 50 ng mL^{-1}, with a detection limit of 16 pg mL^{-1}

Table 1 Determination of ZEN in bovine serum by both methods

Sample[a]	Methods	
	VIS[b]	EIA[c]
BS 1[d]	2.79±0.11[e]	2.81±0.15
BS 2	10.51±0.38	10.32±0.24
BS 3	22.15±0.26	21.97±0.41
BS 4	32.83±0.33	33.28±0.25

[a] Bovine serum samples

[b] Voltammetric immunosensor

[c] Enzyme immunoassay

[d] Bovine Serum and control

[e] Mean of five determinations ± S.D

response must be analyzed. The SWV fixed electrochemical parameters to carry out the optimization of these relevant variables were: step E = 0.010 V, S.W. amplitude = 0.050 V, S.W. frequency = 10 Hz, samples per point = 256, studied potential range = +0.1 to +1.4 V, sensitivity = 1×10^{-5} A V^{-1} using anti-ZEN-AuNPs/MWCNTs-PVP/SPCE as working electrode. Regarding to the ZEN concentration, a standard solution of 25 ng mL^{-1} was employed in all studies.

The amount of polymer deposited on the graphite electrode surface was studied between 0.5 and 4 μL. The current response was linearly increased from 0.5 to 2 μL and then remaining constant. Then, we choose 2.5 μL for the optimal amount of polymer deposited on the electrode surface (Fig. 4a). Another parameter analyzed was the electrodeposition time of the AuNPs which was studied in the range of 10–60 s. The results showed that the signal increased within the first 30 s and then remains constant. Therefore, 30 s was chosen as the optimal electrodeposition time (Fig. 4b). Finally we analyzed the electrodeposition potential of the AuNPs on the electrode surface between −0.1 and −0.6 V being observed an increase in the signal to −0.6 V. Hence we used −0.4 V (Fig. 4c).

The influence of the desorption buffer on the modified electrode response was tested in two different buffer solutions (glycine-HCl and citrate-HCl) in the concentration of 0.1 mol L^{-1} at pH 2.0, obtaining higher I_{pa} responses in glycine-HCl solution (475 nA against 403 nA of citrate-HCl solution). In this sense, glycine-HCl buffer solution was chosen for further studies. The results obtained for the measurements carried out in different concentrations of glycine-HCl buffer (0.01–0.50 mol L^{-1}) showed that I_{pa} values reached a maximum when 0.1 mol L^{-1} was employed and then decreased for solutions with higher concentrations (Online Resource 1). Finally, the pH of glycine-HCl buffer was investigated in the pH range from 1 to 6, obtaining decreased I_{pa} values when the pH increased (Online Resource 2). Thus, 0.1 mol L^{-1} glycine-HCl buffer solution at pH 2.0 was selected as optimum condition for further analyses.

Analytical parameters of anti-ZEN-AuNPs/MWCNTs-PVP/SPCE

The calibration curve for the electrochemical sensing of ZEN was obtained by using the electrochemical immunosensor under optimal experimental conditions. The change of oxidation peak current response of the immunosensor was found to be proportional to the ZEN concentration in a linear range from 0.05 to 50 ng mL^{-1}, with a detection limit of 16 pg mL^{-1}. The data were analyzed by linear regression least-squares fit method. The calibration graph was described by the

Table 2 Comparison with other papers involving modified electrodes with different electrochemical techniques for ZEN determination

Modification	Electrode	Technique	Sample	Linear range (ng mL^{-1})	LOD (pg mL^{-1})
CS-PtCo-Ab/graphene nanosheets [13]	GCE[a]	CV[b]	Urine	0.05–5	13
Na-Mont-TH-HRP-Ab_2/nanoporous gold films-Ab_1 [14]	GCE	A[c]	Liver	0.01–12	3
Graphene sheets-nickel hexacyanoferrate nanocomposites-Ab [15]	GE[d]	A	Liver	0.05–10	6
Gold nanoparticles/poly (vinylpyridine)-multiwalled carbon nanotubes [this work]	SPCE[e]	SVW[f]	Serum	0.05–50	16

[a] Glassy carbon electrode

[b] Cyclic voltammetry

[c] Amperometry

[d] Gold electrode

[e] Screen printed carbon electrode

[f] Square wave voltammetry

calibration equation ΔI_{pa} (nA) = 3.12+19.30 C_{ZEN} with a correlation coefficient for this plot of 0.996, where ΔI_{pa} is the difference between current of the blank and samples (Fig. 4d). The ZEN quantification was directly carried out over diluted samples, and not matrix effects were observed.

Now a day, the possibility of re-use immunosensors is an important characteristic in biosensors field. This immunosensor was regenerated by simply treating with desorption solution for 5 min to dissociate the antibodies-antigen complex. The long-term stability of immunosensor was investigated over a 20 day period, stored at 4 °C. The current response to 25 ng mL^{-1} ZEN maintained about 91 % of the original value after the storage period. The good stability may be attributed to the fact that the immunosensor could provide a biocompatible microenvironment for the antibodies immobilization.

The reproducibility of the immunosensor was studied by intra- and inter-assay. The intra-assay precision was evaluated by assaying the ZEN level for five determinations of one sample in the same day. The intra-assay CV of this method was 4.53 % at ZEN concentrations of 25 ng mL^{-1}. The inter-assay precision was evaluated by determining the ZEN level in one sample along a week. The inter-assay CV was 5.92 % at the ZEN concentration of 25 ng mL^{-1}, showing an acceptable reproducibility.

In order to evaluate the immunosensor response, it was applied to the determination of ZEN in five bovine serum samples under the conditions previously described and the results were compared by enzyme immunoassay. The positive samples were analyzed by our method, which revealed similar concentrations of ZEN in all of them (Table 1). Another important parameter was the analysis time that was only 12 min against the 90 min that takes the enzyme immunoassay technique.

Table 2 summarized and compared the most relevant articles related to modified electrodes with different electrochemical techniques for ZEN determination. It is important to highlight that this is the first electrochemical immunosensor for ZEN determination in bovine serum using a portable SPCE modified with AuNPs/MWCNTs-PVP nanocomposite. Our detection system also used a very sensitive electroanalytical technique such as SWV, combined with anti-ZEN antibodies that provide a high selectivity to the electrochemical sensor. Moreover, in this method we measure the oxidation peak current of ZEN, and the current response was proportional with the concentration in the sample. Finally, the electrochemical method showed an appropriate linear range and LOD for sensing of growth promoter in bovine serum relative to other electrochemical techniques for ZEN determination.

Conclusion

This article described the development of an electrochemical immunosensor for α-zearalanol detection by the construction of a nanostructured functional platform. The AuNPs/MWCNTs-PVP nanocomposite was synthesized using soft conditions and the resulting material showed a good stability. On one hand, an important contribution of this article was demonstrate that even if low conductivity polymers were formed, the contribution of each nanomaterial was clear to enhance the electronic communication and increase the response of the electrode. On the other hand, the developed method showed many advantages like portability, low cost, wide linear range, accuracy with excellent LOD. Another important parameter was the analysis time that was only 12 min against the 90 min that takes the enzyme immunoassay technique. Finally, this method could be a very promising analytical tool for the direct determination of growth promoter in the livestock production, ensuring safety and quality of food, as well as consumer's health.

Acknowledgments The authors wish to thank the financial support from Universidad Nacional de San Luis (UNSL), Instituto de Química de San Luis (INQUISAL), Consejo Nacional de Investigaciones Científicas y Técnicas (CONICET) and Servicio Nacional de Sanidad y Calidad Agroalimentaria (SENASA).

References

1. Bartelt-Hunt SL, Snow DD, Kranz WL, Mader TL, Shapiro CA, Van Donk SJ, Shelton DP, Tarkalson DD, Zhang TC (2012) Effect of growth promotants on the occurrence of endogenous and synthetic steroid hormones on feedlot soils and in runoff from beef cattle feeding operations. Environ Sci Technol 46:1352–1360
2. Wang YK, Yan YX, Mao ZW, Ha W, Zou Q, Hao QW, Ji WH, Sun JH (2013) Highly sensitive electrochemical immunoassay for zearalenone in grain and grain-based food. Microchim Acta 180: 187–193
3. Blokland MH, Sterk SS, Stephany RW, Launay FM, Kennedy DG, Van Ginkel LA (2006) Determination of resorcylic acid lactones in biological samples by GC–MS. Discrimination between illegal use and contamination with fusarium toxins. Anal Bioanal Chem 384: 1221–1227
4. Valenzuela-Grijalva NV, González-Rios H, Islava TY, Valenzuela M, Torrescano G, Camou JP, Núñez-González FA (2012) Changes in intramuscular fat, fatty acid profile and cholesterol content induced by zeranol implantation strategy in hair lambs. J Sci Food Agric 92: 1362–1367
5. Matraszek-Zuchowska I, Wozniak B, Zmudzki J (2013) Determination of zeranol, taleranol, zearalanone, α-zearalenol, β-zearalenol and zearalenone in urine by LC-MS/MS. Food Addit Contam Part A-Chem 30:987–994
6. Roy JR, Chakraborty S, Chakraborty TR (2009) Estrogen-like endocrine disrupting chemicals affecting puberty in humans–A review. Med Sci Monitor 15:137–145
7. Council Directive 88/146/EEC (1988) Off J Eur Commun 70:16–18
8. Sánchez Arribas A, Bermejo E, Zapardiel A, Téllez H, Rodríguez-Flores J, Zougagh M, Ríos Á, Chicharro M (2009) Screening and

confirmatory methods for the analysis of macrocyclic lactone mycotoxins by CE with amperometric detection. Electrophoresis 30: 499–506
9. Han H, Kim B, Lee SG, Kim J (2013) An optimised method for the accurate determination of zeranol and diethylstilbestrol in animal tissues using isotope dilution-liquid chromatography/mass spectrometry. Food Chem 140:44–51
10. De Baere S, Osselaere A, Devreese M, Vanhaecke L, De Backer P, Croubels S (2012) Development of a liquid–chromatography tandem mass spectrometry and ultra-high-performance liquid chromatography high-resolution mass spectrometry method for the quantitative determination of zearalenone and its major metabolites in chicken and pig plasma. Anal Chim Acta 756:37–48
11. Impens S, Van Loco J, Degroodt JM, De Brabander H (2007) A downscaled multi-residue strategy for detection of anabolic steroids in bovine urine using gas chromatography tandem mass spectrometry (GC–MS3). Anal Chim Acta 586:43–48
12. Välimaa AL, Kivistö AT, Leskinen PI, Karp MT (2010) A novel biosensor for the detection of zearalenone family mycotoxins in milk. J Microbiol Methods 80:44–48
13. Zhu J, Tao X, Ding S, Shen J, Wang Z, Wang Y, Xu F, Wu X, Hu T, Zhu A, Jiang H (2012) Micro-plate chemiluminescence enzyme immunoassay for determination of zeranol in bovine milk and urine. Anal Lett 45:2538–2548
14. Feng R, Zhang Y, Yu H, Wu D, Ma H, Zhu B, Xu C, Li H, Du B, Wei Q (2013) Nanoporous PtCo-based ultrasensitive enzyme-free immunosensor for Zeranol detection. Biosens Bioelectron 42:367–372
15. Feng R, Zhang Y, Li H, Wu D, Xin X, Zhang S, Yu H, Wei Q, Du B (2013) Ultrasensitive electrochemical immunosensor for zeranol detection based on signal amplification strategy of nanoporous gold films and nano-montmorillonite as labels. Anal Chim Acta 758:72–79
16. Xue X, Wei D, Feng R, Wang H, Wei Q, Du B (2013) Label-free electrochemical immunosensors for the detection of zeranol using graphene sheets and nickel hexacyanoferrate nanocomposites. Anal Methods 5:4159–4164
17. Taleat Z, Khoshroo A, Mazloum-Ardakani M (2008–2013) Screen-printed electrodes for biosensing: a review. Microchim Acta
18. Ijima S (1991) Helical microtubules of graphitic carbon. Nature 354: 56–58
19. Pompeo F, Resasco DE (2002) Water solubilization of single-walled carbon nanotubes by functionalization with glucosamine. Nano Lett 4:369–373
20. Shamsipur M, Najafi M, Hosseini MRM (2010) Highly improved electrooxidation of glucose at a nickel (II) oxide/multi-walled carbon nanotube modified glassy carbon electrode. Biogeosciences 77:120–124
21. Qin S, Qin D, Ford WT, Resasco DE, Herrera JE (2004) Functionalization of single-walled carbon nanotubes with polystyrene via grafting to and grafting from methods. Macromolecules 37: 752–757
22. Silva CCeC, Breitkreitz MC, Santhiago M, Crispilho Corrêa C, Tatsuo Kubota L (2012) Construction of a new functional platform by grafting poly (4-vinylpyridine) in multi-walled carbon nanotubes for complexing copper ions aiming the amperometric detection of l-cysteine. Electrochim Acta 71:150–158
23. Banerjee S, Benny TH, Wong SS (2005) Covalent surface chemistry of single-walled carbon nanotubes. Adv Mater 17:17–29
24. Sahoo NG, Rana S, Cho JW, Li L, Chan SH (2010) Polymer nanocomposites based on functionalized carbon nanotubes. Prog Polym Sci 35:837–867
25. Wang J (2012) Electrochemical biosensing based on noble metal nanoparticles. Microchim Acta 177:245–270
26. Pereira SV, Bertolino FA, Messina GA, Raba J (2011) Microfluidic immunosensor with gold nanoparticle platform for the determination of immunoglobulin G anti-Echinococcus granulosus antibodies. Anal Biochem 409:98–104
27. Cai X, Gao X, Wang L, Wu Q, Lin X (2013) A layer-by-layer assembled and carbon nanotubes/gold nanoparticles-based bienzyme biosensor for cholesterol detection. Sens Actuator B-Chem 181:575–583
28. Batra B, Pundir CS (2013) An amperometric glutamate biosensor based on immobilization of glutamate oxidase onto carboxylated multiwalled carbon nanotubes/ gold nanoparticles/chitosan composite film modified Au electrode. Biosens Bioelectron 47:496–501